communications biology

A Nature Portfolio journal

Article

https://doi.org/10.1038/s42003-025-09150-0

Single-cell transcriptomics reveals probiotic reversal of neonatal morphine-induced gene disruptions underlying adolescent pain hypersensitivity

Junyi Tao [1,4] ✉, Danielle Antoine [1,2,4], Richa Jalodia [1], Eridania Valdes [1], Sean Michael Boyles [3], William Hulme [3] & Sabita Roy [1] ✉

Neonatal morphine is commonly administered in the Neonatal Intensive Care Unit (NICU) to manage pain. However, its long-term effects on the neurodevelopment of pain pathways remain a significant concern. The midbrain is a core region that plays a central role in pain processing and opioid-mediated analgesia. Here, we perform single-cell RNA sequencing to study gene expression in 107,427 midbrain single cells from adolescent mice neonatally exposed to either saline, morphine, or morphine with the probiotic *Bifidobacterium infantis* (*B. infantis*) for 5 days starting on postnatal day 6-7. We find broad alterations in transcriptomics within neurons, astrocytes, oligodendrocytes, and microglial cells. Analysis of differentially regulated genes reveals down regulation of HOX genes and upregulation of pathways related to neurotransmitter signaling and pain in those adolescent mice neonatally treated with morphine. Interestingly, neonatal probiotic supplementation mitigates these morphine-induced alterations on the transcriptome. This study presents the first single-cell RNA sequencing dataset of the adolescent midbrain following neonatal morphine exposure and probiotic intervention. These findings offer new insights into the neurodevelopmental impact of early opioid exposure and highlight the therapeutic potential of microbiome-targeted interventions.

Opioid analgesics, such as morphine, are frequently administered in Neonatal Intensive Care Units (NICUs) to manage moderate to severe pain in neonates undergoing surgery or invasive procedures[1,2]. Despite their widespread use, the long-term neurobiological consequences of neonatal morphine exposure (NME) remain a critical area of investigation, as accumulating evidence suggests this practice yields adverse outcomes, including increased vulnerability to substance use disorders later in life[3,4]. Emerging clinical and preclinical evidence indicates that NME may lead to detrimental neurodevelopmental effects, such as altered pain sensitivity[4], changes in locomotor activity, and impairments in cognition and learning[2,5]. Neonates may be exposed to opioids both prenatally, with or without subsequent neonatal opioid withdrawal syndrome (NOWS), and postnatally in the NICU[6]. Importantly, postnatal day (PND) 6–7 in mice corresponds to the late gestational stage in humans (~36–40 weeks)[7], such that our 5-day morphine paradigm encompasses both preterm- and term-equivalent developmental windows.

We previously demonstrated that NME induced persistent thermal and mechanical pain hypersensitivity in both female and male adolescent mice, driven by gut microbial dysbiosis, intestinal barrier dysfunction, and systemic inflammation[8]. Notably, neonatal supplementation with the probiotic *Bifidobacterium infantis* (*B. infantis*) prevented the development of pain hypersensitivity by restoring gut microbial dysbiosis and the associated inflammation. Additionally, bulk RNA sequencing of midbrain tissue revealed upregulation of gene networks related to excitatory signaling and neuroimmune activation, many of which were normalized by probiotic treatment, which implicated the gut-brain axis as a key driver of long-term alterations in pain processing following early-life opioid exposure[8]. As the existing literature suggests that females experience chronic pain at a higher prevalence than males during adolescence[9,10], male adolescents were

[1]Department of Surgery, University of Miami Miller School of Medicine, Miami, FL, USA. [2]Department of Neuroscience, University of Miami Miller School of Medicine, Miami, FL, USA. [3]John P. Hussman Institute for Human Genomics, University of Miami Miller School of Medicine, Miami, FL, USA. [4]These authors contributed equally: Junyi Tao, Danielle Antoine. ✉e-mail: Junyitao@miami.edu; Sabita.Roy@miami.edu

excluded from the study, and the focus was given to the female adolescent murine model.

Despite previous findings, the cellular specificity and mechanistic basis of transcriptional changes in the brain remain poorly understood. The midbrain, which encompasses key nodes such as the periaqueductal gray (PAG) and the ventral tegmental area (VTA), plays a central role in pain modulation and reward circuitry[11,12]. However, bulk tissue analysis cannot capture the molecular heterogeneity within distinct neuronal and glial populations, limiting insight into how NME and gut dysbiosis orchestrate long-lasting changes at the cellular level. A high-resolution approach is required to delineate the specific contributions of midbrain cell types to the enduring neuroinflammatory and sensory consequences of neonatal opioid exposure. To fill this knowledge gap, we employed single-cell RNA sequencing (scRNA-seq) to interrogate the transcriptional landscape of over 107,427 individual midbrain cells from adolescent mice exposed to NME, with or without *B. infantis* treatment, alongside saline controls. This high-resolution approach enabled the identification of specific cell types affected by NME and revealed disrupted signaling pathways within each population. Moreover, it provided insight into how microbiome-based interventions may restore gene expression patterns associated with pain hypersensitivity and neurodevelopmental dysfunction following early opioid exposure.

Results

Neonatal morphine exposure and probiotic supplementation did not alter the overall cellular composition of the adolescent mouse midbrain

This study investigated the long-term effects of neonatal morphine exposure on cell-type-specific transcriptional changes in the adolescent mouse midbrain using a murine model. Newborn mice were administered morphine at a concentration of 5 mg/kg/day or saline for five days (Fig. 1A). A separate group of neonatally morphine-exposed mice received supplementation with the probiotic *B. infantis* (Fig. 1A). Single-cell RNA sequencing (scRNA-seq) libraries were generated from 13 mouse midbrains. Midbrains were dissected from mice in the saline (Sal), morphine (Mor), and morphine plus probiotic (Mor+Pro) groups. These tissues were then dissociated into single-cell suspensions and fixed with formaldehyde. Multiplexing antibody barcodes facilitated the sequencing of multiple samples per channel. Cells were captured using the 10X Chromium platform, followed by Illumina sequencing, read alignment, and processing with 10X Cellranger (Fig. 1B). Following doublet removal, quality control filtering, and data integration (see "Methods" and Fig. S1B, C), a total of 107,427 single cells with complete transcriptional profiles were obtained. These cells were subsequently clustered using Seurat and assigned to 13 distinct cell types using the Sc-type pipeline, which integrates data from the CellMarker[13] database and PanglaoDB[14] (Fig. 1C).

Next, we investigated whether neonatal morphine exposure altered the proportions of different cell types in the adolescent midbrain. Across all three experimental groups, neurons constituted approximately 40% of the total cell population. Oligodendrocytes and oligodendrocyte precursor cells (OPCs) combined accounted for 26%, followed by astrocytes (14%), epithelial cells (6%), and microglia (5%), with the remaining cell types each representing less than 5% of the total cell count (Fig. S1A). A Kruskal-Wallis test was performed to determine if any cell type proportions differed significantly among the three conditions. This analysis revealed no significant differences ($p > 0.05$) in the proportions of most cell types across the groups, with the exception of tanycytes ($p = 0.008$) (Fig. 1D). Consistent with this finding, Uniform Manifold Approximation and Projection (UMAP) plots showed highly similar distributions of cell types across the Sal, Mor, and Mor+Pro groups (Fig. S1D).

Neonatal morphine exposure altered the expression of thousands of gene transcripts, in particular HOX genes, in several cells of the adolescent midbrain

We first analyzed cell-type-specific differentially expressed genes (DEGs) to investigate transcriptional changes induced by morphine (Mor vs. Sal) (Supplementary Data 1). Under the morphine condition, each cell type displayed distinct changes, as illustrated in the combined volcano plots (Fig. 2A). Specifically, more than one thousand DEGs were identified in glutamatergic and GABAergic neurons, oligodendrocytes, and astrocytes. In contrast, fewer than five hundred DEGs were observed in microglia, OPCs, and cholinergic neurons (Fig. 2B). An upset plot (Fig. 2B) revealed that most DEGs were unique to each cell type. Glutamatergic and GABAergic neurons, oligodendrocytes, and astrocytes each had over 500 unique DEGs, whereas microglia, OPCs, and cholinergic neurons had fewer than 200. Notably, a set of HOX genes exhibited significant downregulation, with the lowest Log2 fold change in glutamatergic and GABAergic neurons, oligodendrocytes, and astrocytes under morphine conditions (Fig. 2A).

Neonatal morphine exposure induced canonical pathway changes, including neurotransmitter signaling and cellular growth and proliferation in the midbrain

To further investigate genome-wide alterations in gene transcripts, we performed a QIAGEN IPA canonical pathway enrichment analysis, focusing on cell types with the highest number of DEGs (Supplementary Data 2). We then generated enrichment bubble plots for glutamatergic neurons, GABAergic neurons, astrocytes, and oligodendrocytes (Fig. S2) and a summary heatmap (Fig. 3). Under morphine conditions (Mor vs. Sal), several canonical pathways, including gene transcription, signal transduction, cell growth and proliferation, and neurotransmitter signaling, were significantly upregulated in glutamatergic neurons (Fig. 3, S2A). Similarly, in GABAergic neurons, signal transduction, cellular growth and proliferation, and neurotransmitter signaling were upregulated under morphine conditions (Fig. 3, S2B). In astrocytes, under morphine conditions, we observed increased metabolism, neurotransmitter signaling, organismal growth and development, and disease-specific pathways (Fig. 3, S2C). Under morphine conditions, oligodendrocytes showed increased neurotransmitter signaling, biosynthesis, disease pathways, and cellular stress and injury (Fig. 3, S2D).

Probiotic supplementation reversed the expression of HOX genes in specific cell types induced by neonatal morphine exposure in the midbrain

Previous studies from our group have shown that neonatal probiotic intervention with *B. infantis* reversed the pain hypersensitivity and mitigated NME-induced transcriptional changes in the midbrain by attenuating gut dysbiosis[8]. Therefore, to assess the impact of gut microbiome-targeted intervention, we analyzed cell-type-specific DEGs under probiotic supplementation (Mor+Pro vs. Mor) and compared them to the saline control (Mor+Pro vs. Sal). Interestingly, HOX genes downregulated under morphine conditions showed significant upregulation with probiotic supplementation. However, this reversal was specific to glutamatergic and GABAergic neurons, oligodendrocytes, astrocytes, and OPCs (Fig. 4, S3). In glutamatergic and GABAergic neurons, probiotic supplementation led to a 64-fold increase (6 units of Log2 fold change increase) of HOX genes (Fig. 4A, B). However, when compared to saline control, HOX genes were still downregulated with a log2 fold change of -4, suggesting the probiotic supplementation did not completely reverse the downregulation of HOX genes. In astrocytes and oligodendrocytes, probiotic supplementation similarly caused a 64-fold increase in gene expression (Fig. 4C, D). Interestingly, when compared to saline control, HOX genes were no longer among the most regulated genes, suggesting that probiotic supplementation successfully reversed the downregulation of HOX genes. In OPCs, probiotic supplementation induced a smaller increase of HOX genes and was able to reverse the downregulation of HOX genes from morphine (Fig. S3A). In contrast, HOX genes were not downregulated in microglia and cholinergic neurons under morphine conditions nor did probiotic supplementation lead to increased HOX gene expression (Fig. S3B, C).

Probiotic supplementation reversed canonical pathway changes that were induced by neonatal morphine exposure in the midbrain

To further investigate the impact of probiotic supplementation on canonical pathways, we performed a QIAGEN IPA canonical pathway enrichment

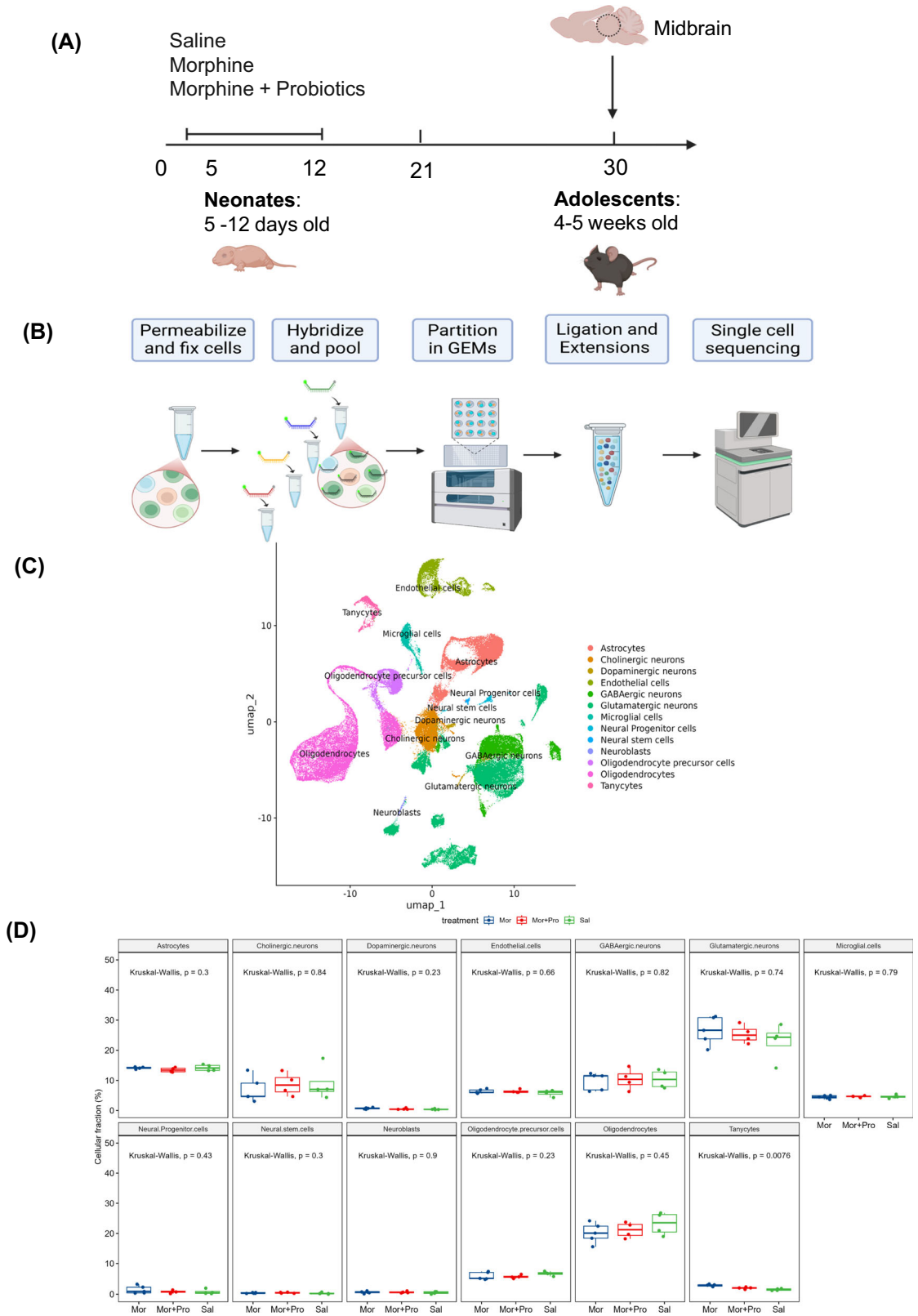

Fig. 1 | Consistent proportions of cell types across treatment groups. A, **B** Animal treatment design and single-cell workflow for 13 samples. Saline ($n = 4$), Morphine ($n = 5$), Morphine+Probiotics ($n = 4$). Created with BioRender.com (**C**). Uniform Manifold Approximation and Projection (UMAP) plot showing the identified 13 major cell types, for a total of $n = 107{,}427$ cells. **D** Box plot of the 13 major cell types in each sample, split by treatment group. See also Figure S1, Supplementary Data 4.

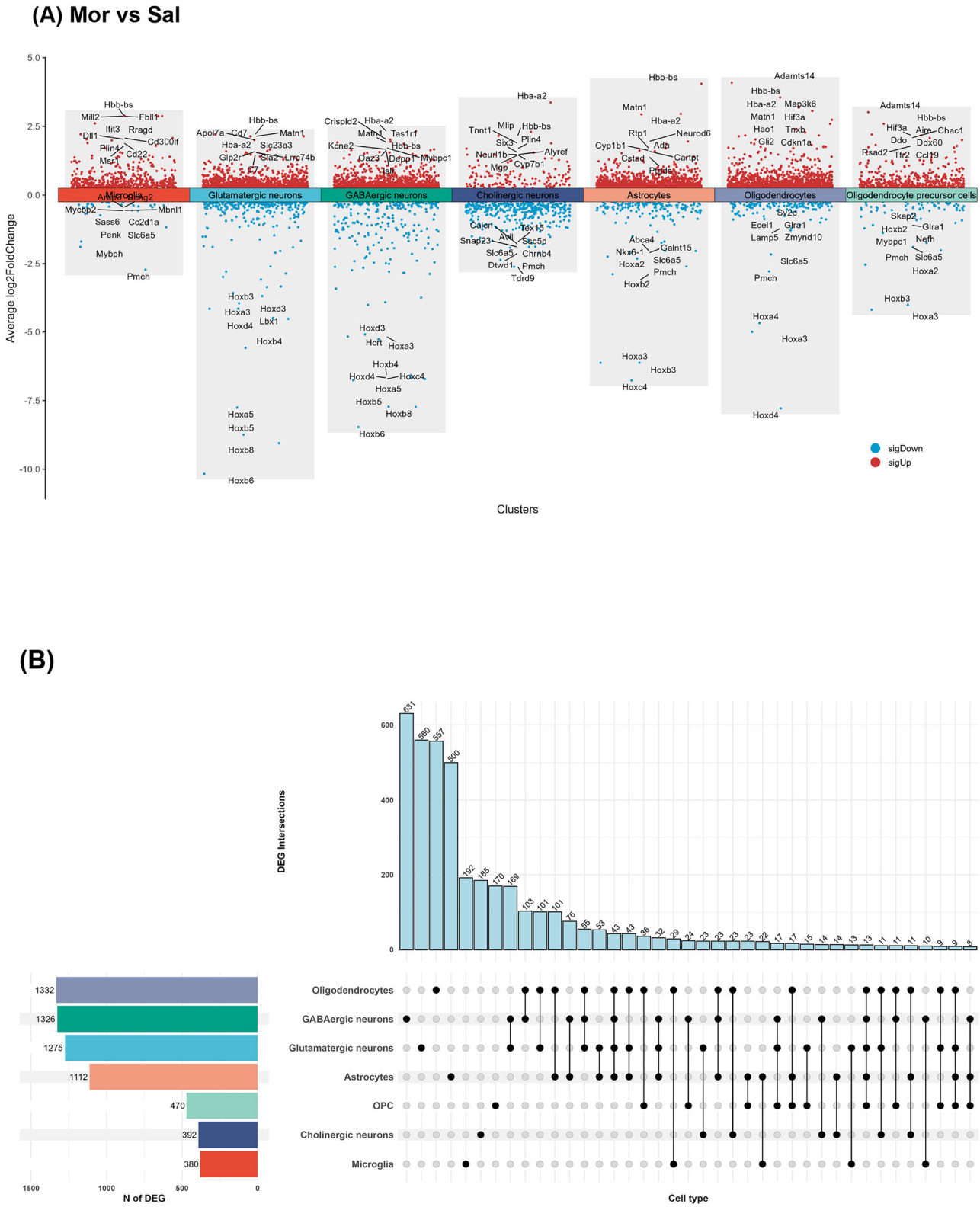

Fig. 2 | Differentially expressed genes (DEGs) under Mor vs Sal. A Combined volcano plot representation of differentially expressed genes (DEGs) across cell types. **B** UpSet diagram represents counts of shared DEGs across cell types and number (*N*) of DEGs for each cell type. Genes with |Log2FC| > 0.25 and adjusted *p* value < 0.005 are counted as significantly changed. See also Supplementary Data 1.

analysis under probiotic supplementation (Mor+Pro vs. Mor), focusing on glutamatergic neurons, GABAergic neurons, astrocytes, and oligodendrocytes (Fig. 3, S4). Under probiotic supplementation (Mor+Pro vs. Mor), the majority of pathways that were upregulated by NME were downregulated in glutamatergic neurons (Fig. 3, S4A), with neurotransmitter signaling, cellular growth and development, and cellular immune response among the most significantly downregulated. Similarly, in GABAergic neurons, probiotic supplementation led to the downregulation of neurotransmitter signaling, organismal growth and development, transcription regulation, and cell stress and injury (Fig. 3, S4B). In astrocytes, probiotic

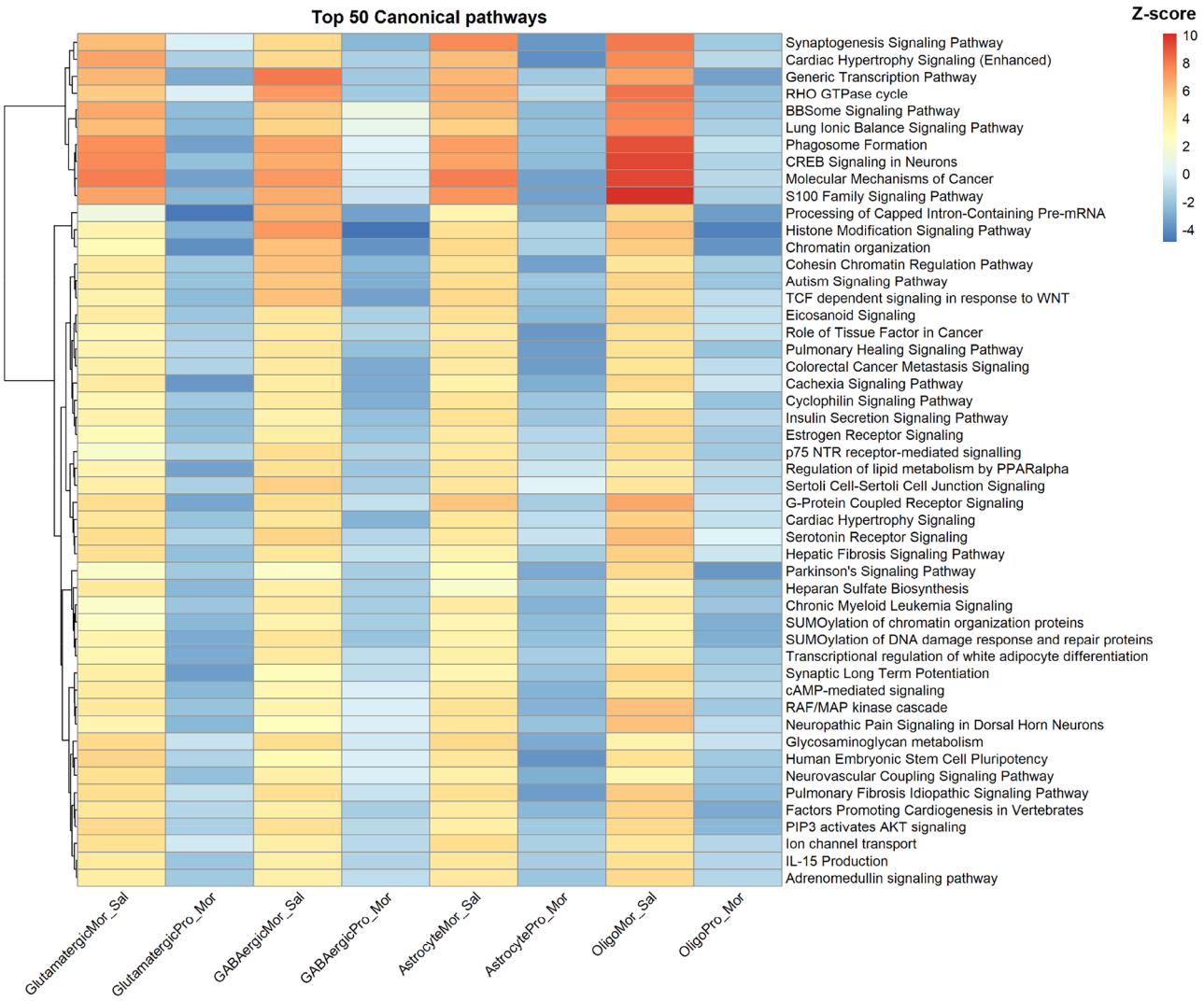

Fig. 3 | Canonical pathway changes induced by neonatal morphine exposure and probiotics. Heatmap of Top 50 canonical pathways for glutamatergic neurons under Mor vs Sal and Mor+pro vs Mor conditions. GABAergic neurons under Mor vs Sal and Mor+pro vs Mor conditions. Astrocytes under Mor vs Sal and Mor+pro vs Mor conditions. Oligodentrocytes under Mor vs Sal and Mor+pro vs Mor conditions. Values are expressed in IPA z-scores. See also Supplementary Data 2.

supplementation resulted in the downregulation of disease-specific pathways, neurotransmitter signaling, and cell stress and injury in astrocytes (Fig. 3, S4C). Probiotic supplementation in oligodendrocytes led to decreased biosynthesis, intracellular signaling, degradation utilization, and gene transcription (Fig. 3, S4D).

Neonatal morphine exposure enhanced neuropathic pain pathways, while probiotic supplementation attenuated them

Previous studies from our group have shown that NME induces prolonged pain hypersensitivity during adolescence[8], Therefore, we investigated how pain-related canonical pathways were affected by morphine and probiotic supplementation in specific cell types.

Glutamatergic neurons play a significant role in neuropathic pain. Under morphine conditions (Mor vs. Sal), these neurons exhibited enhanced overall neuropathic pain pathways (Fig. 5A). Specifically, multiple subunits of Metabotropic Glutamate Receptors (mGluR-GRM), Ionotropic Glutamate Receptors AMPA type (GRIA – AMPA), and Ionotropic Glutamate Receptors NMDA type (NMDA) were upregulated (Fig. S6A). However, probiotic supplementation (Mor+Pro vs. Mor) attenuated these pain pathways in glutamatergic neurons (Fig. 5B). Most glutamate transporter genes were downregulated, including mGluR-GRM and NMDA receptors (Fig. S6B). No significant changes in pain pathways were observed in inhibitory GABAergic neurons. Astrocytes also modulate neuropathic pain through interactions with neurons and other glial cells. Similar to glutamatergic neurons, astrocytes showed enhanced neuropathic pain pathways under morphine conditions (Fig. 5C) and decreased pain pathways with probiotic supplementation (Fig. 5D). Similarly, mGluR-GRM and NMDA receptors were upregulated with morphine (Fig. S6C) and downregulated with probiotic supplementation (Fig. S6D). Oligodendrocytes displayed a similar trend of increased and decreased neuropathic pain pathways with morphine exposure and probiotic supplementation, respectively (Fig. S5, S6E, F).

Neonatal morphine exposure increased cell-cell communication between glutamatergic neurons, astrocytes, and oligodendrocytes, and probiotic supplementation attenuated this communication

Next, we analyzed cell-cell communication using CellChat (see Methods) among glutamatergic neurons, astrocytes, and oligodendrocytes, to investigate how cell communication was affected by morphine and probiotic supplementation. We first compared the number and strength of these interactions between glutamatergic neurons, astrocytes, and oligodendrocytes to identify significant changes under morphine and probiotic conditions. Based on circle plots (Fig. 6A, S7A), both the number and

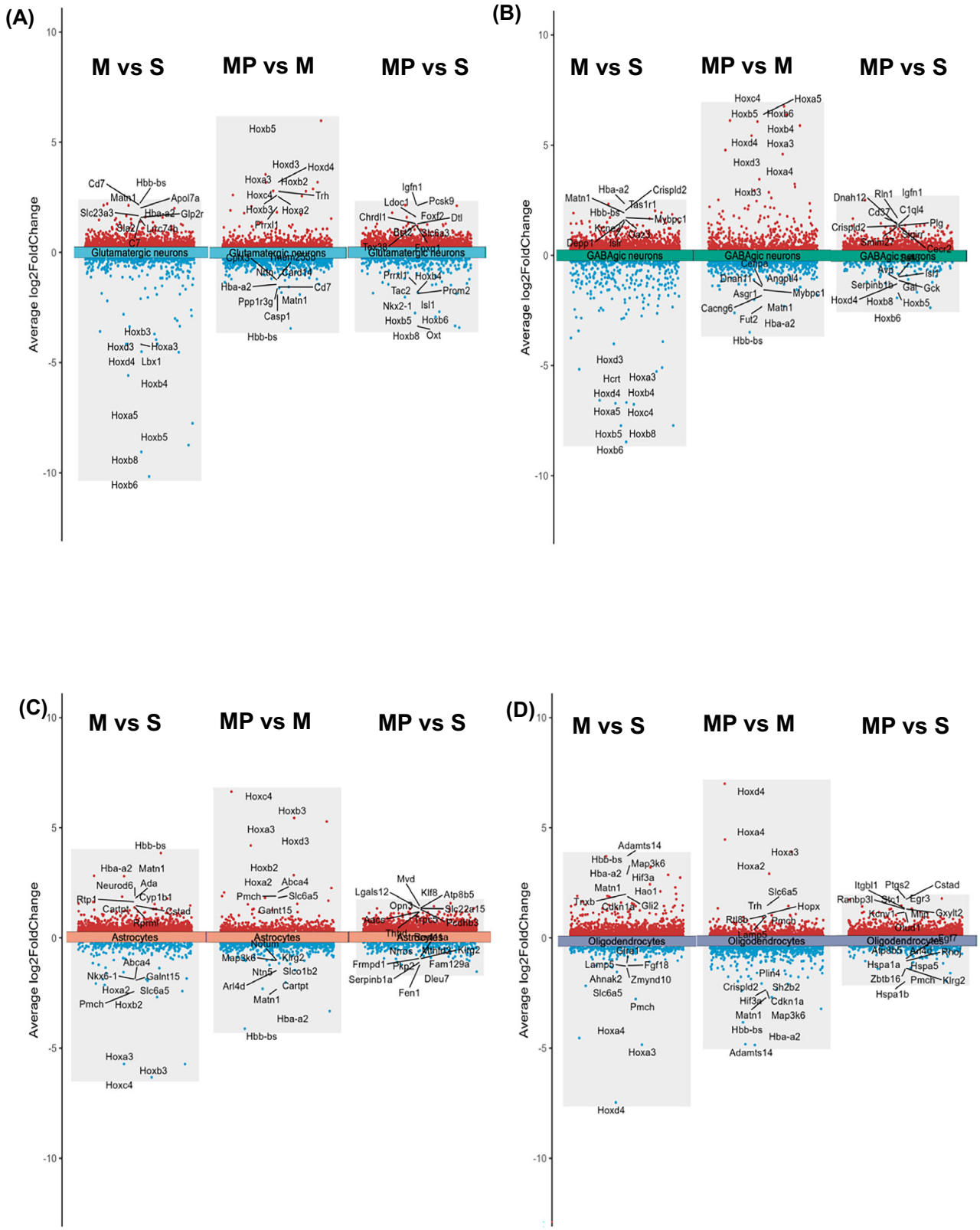

Fig. 4 | Differentially expressed genes (DEGs) under Mor vs Sal and Mor+Pro vs Mor. Side-by-side DEGs comparisons of Glutamatergic neurons (**A**), GABAergic neurons (**B**), astrocytes (**C**), and oligodendrocytes (**D**) in Mor vs Sal, Mor+Pro vs Mor, and Mor+Pro vs Sal conditions. Genes with |Log2FC| 0.25 and adjusted *p*-value 0.05 are counted as significantly changed. M vs S, morphine vs saline. MP+M, morphine+probiotics vs morphine. MP vs S, morphine+probiotics vs saline. See also Fig. S3 and Supplementary Data 1.

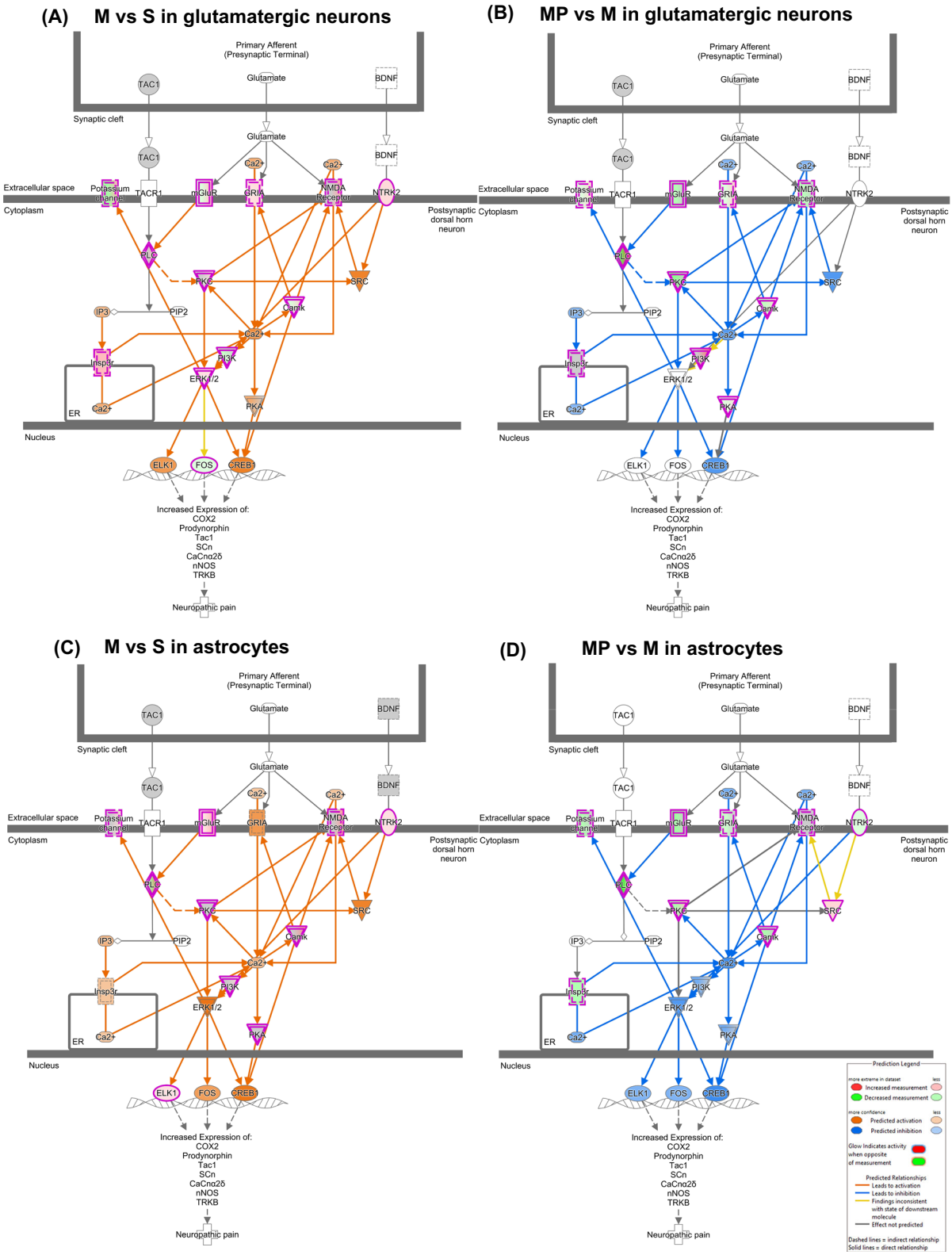

Fig. 5 | Neuropathic pain pathways changes induced by neonatal morphine exposure and probiotics. Neuropathic pain pathways of glutamatergic neurons under Mor vs Sal (**A**) and Mor+Pro vs Mor (**B**) conditions. Astrocytes under Mor vs Sal (**C**) and Mor+Pro vs Mor (**D**) conditions. M vs S, morphine vs saline. MP+M, morphine+probiotics vs morphine. See also Figs. S5 and S6.

strength of interactions from glutamatergic neurons to glial cells increased under morphine conditions (Mor vs. Sal). Similarly, the number and strength of interactions from glial cells to glutamatergic neurons also increased (Fig. 6A, S7A), indicating bidirectional enhancement of cell-cell communication with morphine exposure. Under probiotic supplementation (Mor+Pro vs. Mor), we observed a reversal of these trends; both the number and strength of interactions from glutamatergic neurons to glial cells decreased (Fig. 6B, S7B), as did the communication from glial cells to glutamatergic neurons (Fig. 6B, S7B), suggesting that probiotic treatment reduced bidirectional communication between these

cell types. Next, we conducted information flow analysis to identify signaling pathways altered by the different conditions, by calculating the sum of communication probabilities among all ligand-receptor pairs within the inferred network. Under morphine conditions (Mor vs. Sal), glutamate and neurexin (NRXN) pathways showed increased overall information flow from glutamatergic neurons to astrocytes and oligodendrocytes (Fig. 6C). However, under probiotic supplementation (Mor+Pro vs. Mor), these pathways exhibited reduced information flow from glutamatergic neurons to astrocytes and oligodendrocytes (Fig. 6D). Similarly, morphine exposure increased information flow of glutamate and NRXN pathways from astrocytes and oligodendrocytes to glutamatergic neurons (Fig. S7C), while probiotic treatment decreased this information flow (Fig. S7D).

Upstream regulator analysis indicated that retinoic acid receptors (RARs) were downregulated by neonatal morphine exposure and upregulated by probiotic supplementation

Finally, we performed IPA Upstream Regulator Analysis to identify the potential upstream regulator mechanism based on the observed gene expression changes in our scRNA-seq dataset (Supplementary Data 3). Given the significant fluctuations in HOX gene expression observed in specific cell types under morphine and probiotic conditions (Fig. 4), we focused our analysis on these genes to determine their regulatory relationships. Specifically, under morphine conditions (Mor vs. Sal), Retinoic acid receptors (RARs) alpha and gamma were predicted to be significantly downregulated in glutamatergic neurons (Fig. 7A, S8A). Furthermore, RAR/retinoid X receptor (RXR) heterodimers also showed predicted lower expression under morphine conditions (Fig. S8A). Conversely, RAR-alpha, RAR-gamma, and the RAR/RXR complex were all predicted to be significantly upregulated in glutamatergic neurons with probiotic supplementation (Mor+Pro vs. Mor) (Fig. 7B, S8B). Similarly, in GABAergic neurons under morphine conditions, RAR-alpha and RAR-gamma were predicted to be significantly downregulated (Fig. 7C, S8C). However, probiotic supplementation led to the predicted upregulation of RAR-alpha, RAR-gamma, and the RAR/RXR complex in GABAergic neurons (Fig. 7D, S8D). In astrocytes under morphine conditions, only RAR-alpha was predicted to be significantly downregulated (Fig. 7E). Probiotic supplementation, however, was associated with the predicted upregulation of RAR-alpha, RAR-beta, and RAR-gamma in astrocytes (Fig. 7F, S9). Finally, in oligodendrocytes, RAR-alpha was the sole regulator predicted to be downregulated under morphine conditions and upregulated with probiotic supplementation (Fig. 7G, H).

Discussion

This study presents the first single-cell RNA sequencing dataset of the adolescent mouse midbrain following neonatal morphine exposure and probiotic intervention. Using a murine model, we found that NME induced cell-type-specific changes in gene expression, disrupted canonical signaling pathways, and altered cell-cell communication in the adolescent midbrain. Notably, probiotic supplementation with *B. infantis* reversed many of these morphine-induced alterations in gene expression, including those related to pain pathways and cell-cell communication. These findings offer novel insights into the long-term impact of early opioid exposure on the brain and highlight potential mechanisms through which microbiome-targeted therapies may exert neuroprotective effects.

We found that neonatal morphine treatment did not significantly alter the proportions of most midbrain cell types. However, it disrupted gene expression profiles across multiple populations. Specifically, glutamatergic and GABAergic neurons, oligodendrocytes, and astrocytes had the greatest number of DEGs overall and unique DEGs. These findings are consistent with prior single-cell studies. For instance, a previous single-cell study showed that while the proportion of each cell type was consistent and chronic morphine treatment did not influence the composition of the amygdala tissue, the treatment did affect the transcriptional profiles of all cell types[15]. In that study, microglia, endothelial cells, neurons, and oligodendrocyte progenitor cells had the greatest number of up- and down-regulated genes[15]. Similarly, in a human study, single-cell transcriptomics of postmortem midbrain tissue from individuals with a history of opioid use revealed that microglia, oligodendrocytes, OPCs, and astrocytes accounted for the majority of DEGs[16]. In that study as well, chronic opioid exposure and overdose were not associated with proportional shifts among the neuronal and glial constituents[16]. A separate study in human striatal tissue from individuals with opioid use disorder (OUD) found no significant differences in the proportions of neuronal and glial cell types, but identified 1,765 DEGs across cell types, with glial cells showing more transcriptional changes than neurons[17]. Taken together, these findings support a model in which opioid exposure alters cell-type-specific transcriptional programs without significantly affecting cellular composition. Variability across studies may reflect differences in opioid treatment regimens, single-cell sequencing techniques, or confounding factors in human subjects.

Additionally, we found that neonatal morphine exposure upregulated various canonical pathways related to neurotransmitter signaling, cellular growth, immune response, and disease-related pathways. These findings are consistent with our current understanding of opioid-induced neuroinflammation[18,19] and align with bulk RNA-sequencing data from our previous work using the same animal model[8]. Moreover, our results demonstrated that neurotransmitter signaling and cellular immune response, along other pathways that were previously upregulated with neonatal morphine exposure, were downregulated by probiotic intervention. Prior studies have reported similar pathway alterations in response to opioid treatment. For example, in the amygdala, chronic morphine exposure was shown to upregulate pathways related to cell activation, immune and inflammatory responses, cytokine signaling, and metabolic processes[15]. In postmortem human ventral midbrain tissue, glial cell populations, including astrocytes, pericytes, microglia, and oligodendrocytes, exhibited strong upregulation of immune-related pathways, including interferon signaling, NF-κB activation, and cell motility[16]. In the striatum of individuals with OUD and opioid-exposed rhesus macaques, neurons showed enrichment of pathways linked to neurodegeneration, interferon responses, and DNA damage, while glial cells displayed upregulation of neuroinflammation and synaptic signaling pathways[17]. Furthermore, a single-nucleus RNA-seq study of brain organoids derived from patients with OUD found that oxycodone induced type I interferon signaling in neurons and astrocytes, whereas buprenorphine activated the mTOR pathway in astrocytes[20]. However, these previous studies did not examine therapeutic interventions and thus provide no data on the potential modulatory effects of probiotics. Our findings fill this gap by demonstrating that microbiome-targeted treatment can reverse morphine-induced transcriptional and pathway-level changes.

One of the most striking findings from our study was the morphine-induced downregulation of homeobox (Hox) genes across multiple midbrain cell types. Hox genes are highly conserved developmental transcription factors that play essential roles in establishing positional identity, regional specification, tissue patterning, and cell differentiation[21,22]. Although direct evidence linking Hox genes to opioid addiction is limited, several of these genes have been implicated in nociceptive circuit formation in the spinal cord, particularly relevant given our prior observation that NME leads to persistent pain hypersensitivity during adolescence[8]. Hox genes are critically involved in the formation of the hindbrain and spinal cord, where they regulate the identity and connectivity of spinal interneurons involved in pain processing.[23–26]. The expression of distinct combinations of Hox genes in the hindbrain rhombomeres is required to generate the precursors of visceral sensory interneurons[27]. Additionally, loss of *Hoxb8* in a murine model led to excessive lower back grooming, localized skin lesions in adult mutant mice, and attenuated responses to nociceptive and thermal stimuli[28]. Importantly, several studies revealed connectivity defects in spinal cord circuits upon Hox gene inactivation. For example, early or late genetic removal of *Hox5* in mice affects diaphragm innervation, demonstrating that *Hox5* genes are required for proper connectivity of phrenic motor neurons to premotor interneurons[29]. *Hoxc8* removal specifically in sensory neurons affects sensory-motor connectivity[30] whereas

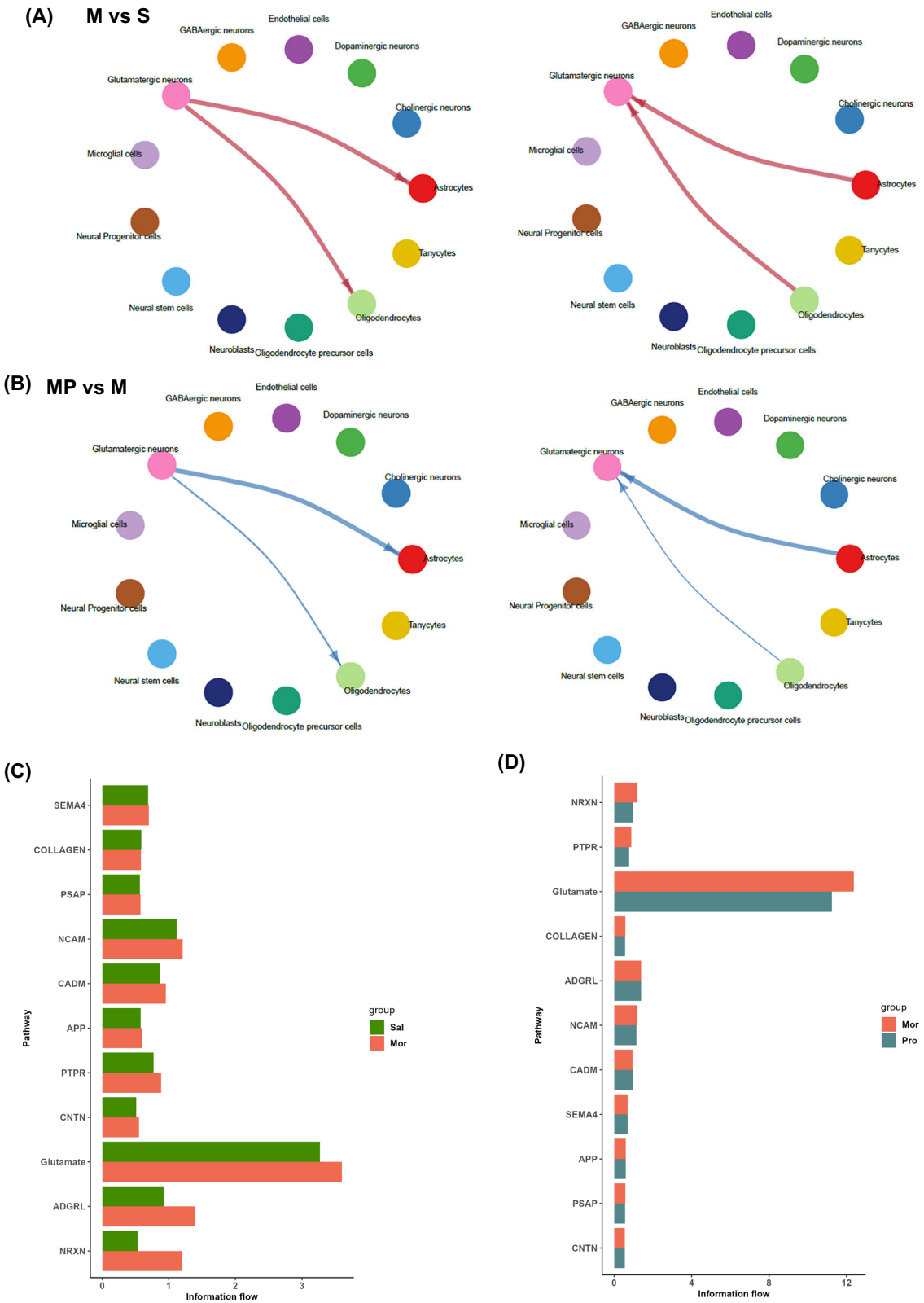

Fig. 6 | cell–cell communication among Glutamatergic neurons, astrocytes and oligodendrocytes. A Circle plot showing a differential number of interactions between Glutamatergic neurons, astrocytes, and oligodendrocytes under M vs S. Red (or blue) colored edges represent increased (or decreased) signaling in the comparison. **B** Circle plot showing differential number of interactions between Glutamatergic neurons, astrocytes, and oligodendrocytes under MP+M. **C** Overall information flow of top signaling pathway from Glutamatergic neuron to astrocytes and oligodendrocytes under M vs S. **D** Overall information flow of top signaling pathway from Glutamatergic neuron to astrocytes and oligodendrocytes under MP +M. M vs S, morphine vs saline. MP+M, morphine +probiotics vs morphine. See also Fig. S7.

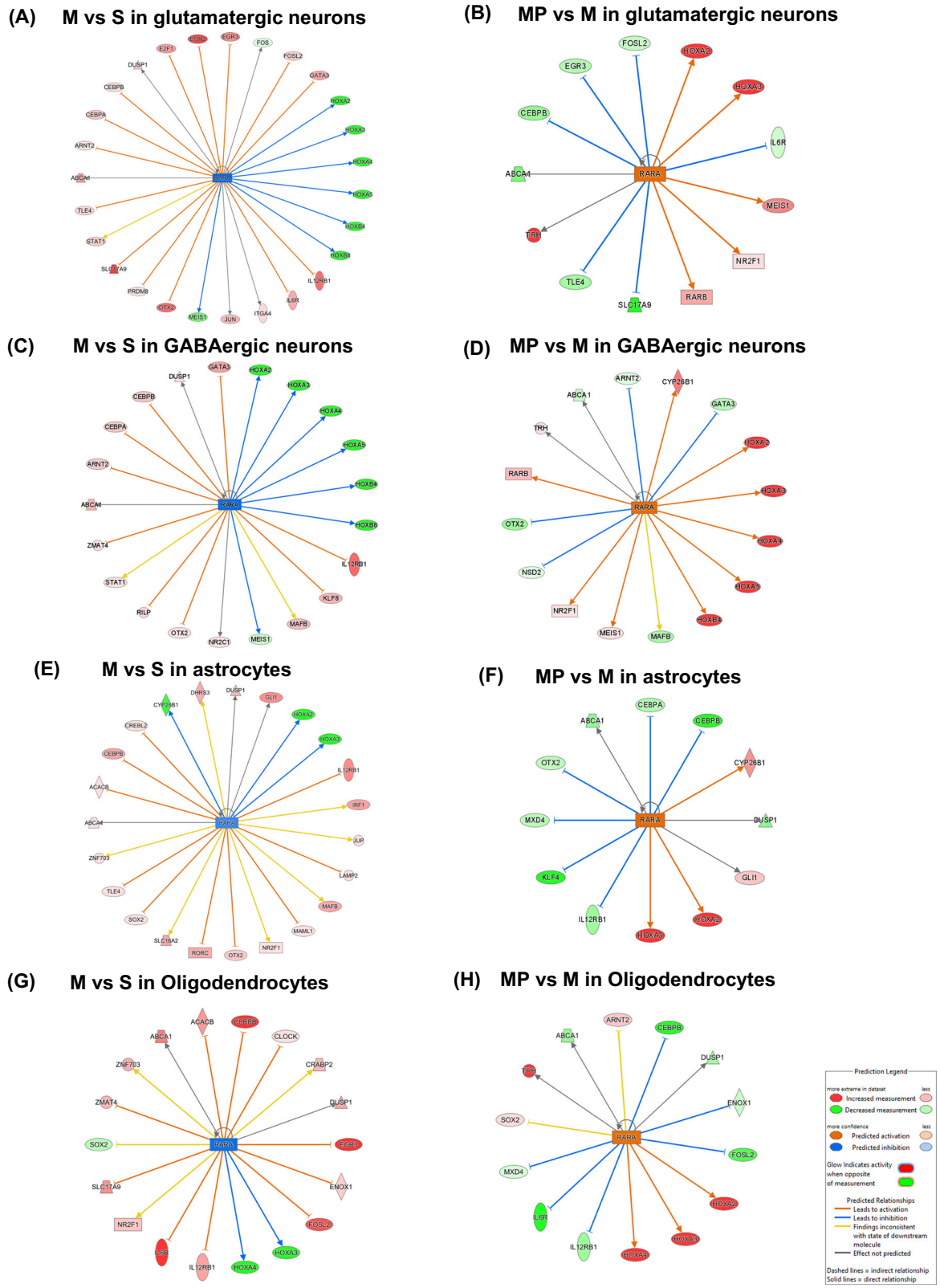

Fig. 7 | Retinoic acid receptors (RARs) downregulated by neonatal morphine exposure and upregulated by probiotic supplementation. IPA upstream regulator analysis of glutamatergic neurons under Mor vs Sal (**A**) and Mor+Pro vs Mor (**B**) conditions, GABAergic neurons under Mor vs Sal (**C**) and Mor+Pro vs Mor (**D**) conditions, Astrocytes under Mor vs Sal (**E**) and Mor+Pro vs Mor (**F**) conditions., Oligodendrocytes under Mor vs Sal (**G**) and Mor+Pro vs Mor (**H**) conditions. M vs S, morphine vs saline. MP+M, morphine+probiotics vs morphine. See also Figs. S8, S9, and Supplementary Data 3.

motor neuron-specific depletion of *Hoxc8* affects forelimb muscle innervation[31]. These studies highlight that Hox genes are important in establishing and maintaining normal neuronal wiring and synaptic plasticity during the post-natal stages. But importantly, our data show that probiotic supplementation restored the expression of several Hox genes across diverse midbrain cell types. This restoration included a partial reversal of Hox gene expression in glutamatergic and GABAergic neurons, while a complete reversal was observed in oligodendrocytes, astrocytes, and OPCs. The observed difference in the response to probiotics between neuronal and glial cells could be attributed to a dose-dependent effect. Given that morphine induced a more significant downregulation of Hox genes in neurons than in glial cells (a Log2 fold change of -10 versus -6, respectively), a higher probiotic dose or a longer duration of treatment might be necessary to achieve a complete reversal of gene expression in glutamatergic and GABAergic neurons. Alternatively, the difference could reflect a ceiling effect of the probiotic's impact. Since Hox gene downregulation was more pronounced in neurons, the current probiotic treatment alone may not be sufficient to achieve full reversal, suggesting a limit to its restorative capacity under these conditions. Given the role of Hox genes in specifying, differentiating, and refining synaptic connections in pain-related neurons, their reactivation may represent a key mechanism through which probiotics counteract morphine-induced neurodevelopmental disruption. These results not only reinforce the critical role of Hox gene expression in maintaining neuronal function but also suggest that microbiome-targeted interventions can reverse opioid-induced transcriptional dysregulation and support neurodevelopmental resilience.

In addition to the observed homeobox gene disruptions, IPA analysis of our single-cell transcriptomic data revealed a coordinated upregulation of the neuropathic pain signaling pathway across multiple midbrain cell types following neonatal morphine exposure. Specifically, morphine-treated mice exhibited increased expression of glutamate receptor genes, including metabotropic glutamate receptors (mGluRs), AMPA receptors (GRIA), and NMDA receptors (GRN). These receptors regulate synaptic excitability and plasticity[32], and their upregulation under morphine conditions may contribute to central sensitization processes[33–35]. However, glutamate receptor activation also exerts broad neurodevelopmental effects beyond nociception, including roles in learning, memory, and synaptic refinement. Thus, our findings indicate a morphine-induced shift toward hyperexcitability and maladaptive plasticity, which may underlie, but may not be limited to, pain-related outcomes. Additionally, morphine exposure led to increased expression of key neurotrophin-related molecules, such as the neurotrophin receptor *NTRK2* (TrkB), which mediates brain-derived neurotrophic factor (BDNF) signaling. This pathway is known to enhance neuronal excitability[36]. We also identified upregulation of multiple intracellular signaling cascades, including phospholipase C (PLC), protein kinase C (PKC), calmodulin-dependent kinase (CaMK), phosphoinositide 3-kinase (PI3K), and extracellular signal-regulated kinases 1/2 (ERK1/2), all of which converge on transcriptional regulators like *CREB1* and *ELK1* to promote the long-term transcriptional programs sustaining chronic pain states[37–39]. These changes were accompanied by predicted increases in intracellular calcium signaling (Ca^{2+}, *IP3*, *IP3R*) and kinase activity (*SRC*, *PKA*), further indicating a morphine-induced shift toward hyperexcitability and maladaptive plasticity. Remarkably, probiotic supplementation reversed the expression direction of nearly all these genes and predicted signaling events in multiple cell types, including glutamatergic neurons, astrocytes, and oligodendrocyte lineage cells. This reversal suggests that the probiotic both mitigates transcriptional dysregulation associated with pain sensitization and may also restore homeostatic signaling in critical neurodevelopmental and neuromodulatory pathways. These findings are consistent with prior studies demonstrating the role of opioid-induced microbial dysbiosis in morphine-associated comorbidities and the potential of probiotics to ameliorate such effects[8,40,41]. For example, probiotic VSL#3, containing several *Bifidobacterium* and *Lactobacillus* species, has been shown to prevent the development of morphine tolerance by restoring microbial balance[40]. Similarly, Cai et al. reported that gut microbiota from fibromyalgia patients induced pain behavior in mice, which was reversed by microbiota from healthy individuals, suggesting a causal role for microbiota in widespread pain[42]. In our previous study, we demonstrated that *B. infantis* supplementation in neonates mitigated pain hypersensitivity by restoring gut microbial composition and reducing systemic inflammation.[8] The present study extends those findings by showing that *B. infantis* can also rescue morphine-induced transcriptional disruptions at the single-cell level. Together, these findings position probiotic intervention as a promising strategy to attenuate early-life morphine-induced molecular reprogramming that contributes to neurodevelopment deficits. Moreover, our cell-cell communication analysis demonstrated that there was a bidirectional increase in communications among glutamatergic neurons, astrocytes, and oligodendrocytes under morphine conditions. Particularly, glutamate pathway communication which was involved in pain signaling was among the most increased pathway under the morphine condition. Probiotic supplementation was able to decrease bidirectional communication among cells as well as the glutamate pathway. The cell-cell communication analysis results, along with pain pathway analysis, corroborate our previous findings that neonatal supplementation with the *probiotic B. infantis* prevented the onset of pain hypersensitivity[8].

Finally, our upstream regulator analysis revealed that RARs and RXRs can be potential regulators during neonatal morphine exposure and probiotic supplementation. RARs are a type of nuclear receptor that act as ligand-activated transcription factors. They are activated by all-trans-retinoic acid (ATRA), a derivative of vitamin A. There are three main types of RARs of RXRs: RAR-alpha, RAR-beta, and RAR-gamma. RXRs often form heterodimers with other nuclear receptors, including RARs, to regulate gene expression[43]. A multi-omics study of morphine effects on mice reported that all-trans-retinoic acid (atRA) were depleted in the ileal luminal metabolome of the morphine group[44]. Further, their bulk-RNA sequencing of ileum tissue showed a decrease in retinol metabolism as well as a decrease in Retinol Dehydrogenase 7 (Rdh7), which is a key regulator in retinol metabolism. Their results were consistent with our finding that RARs were downregulated with neonatal opioid exposure, and morphine exposure likely disturbed retinol metabolism in the gut, therefore reducing transcription activities by RAR and RAR/RXR. The present study showed that probiotic supplementation could upregulate the RAR and RXR that were downregulated by neonatal opioid exposure. Multiple studies in the field have demonstrated the direct involvement of gut microbiota in vitamin A metabolism. Grizotte-Lake et al.[45] demonstrated a direct role of commensal bacteria in modulating the concentration of the vitamin A metabolite retinoid acid in the gut. They reported that bacteria belonging to class Clostridia suppressed Rdh7 expression and retinoid acid synthesis. Woo et al.[46] found that segmented filamentous bacteria (SFB) and other beneficial commensal bacteria generate intestinal retinoic acid levels despite inhibition of host production. Bonakdar et al.[47] discovered that gut bacteria *Lactobacillus intestinalis* metabolized vitamin A and specifically restored retinoid acid levels in the gut of vancomycin-treated mice. Our previous research showed that NME adolescents mice given *B. infantis* supplementation showed an increase in mainly the commensal genera of *Lactobacillus*, *Bacteroides*, and *Turicibacter*, which may play a role in regulating vitamin A metabolism and RAR/RXR activities[8].

Although this study provides important insight into the molecular and cellular consequences of NME, it has several limitations that warrant consideration. While the use of a murine model allowed for rigorous experimental control and mechanistic insight into the effects of NME and microbiome-targeted interventions, the translational relevance of these findings remains to be established. Future clinical studies are needed to assess whether probiotic supplementation can similarly mitigate opioid-induced neurodevelopmental disruptions in human infants. Moreover, while this study focused primarily on pain-related pathways, early-life opioid exposure has been associated with a broader range of neurobehavioral alterations. Follow-up studies examining additional behavioral domains, such as locomotor activity, learning, and cognition, will be critical to fully elucidate the long-term functional consequences of NME. An

additional limitation is the absence of sex-dependent analyses, as this study was restricted to female midbrain samples. Although we previously found that NME induces hypersensitivity in both sexes, we chose to focus on female mice given evidence that females experience pain more frequently and for longer durations. Future studies should include both sexes to delineate sex-specific molecular and behavioral outcomes. A further limitation is that our work was restricted to a single opioid, morphine, and to a single timepoint, adolescence. While morphine was chosen given its widespread clinical use, and adolescence was the intended developmental window of interest, future studies should expand to other opioids and developmental stages to provide a more comprehensive understanding of early-life opioid exposure. Furthermore, to disentangle the main effects of the probiotic from its interaction with morphine, a probiotic-only treatment group should be included in future study designs. Lastly, our use of the 10x Genomics Chromium Fixed RNA Profiling assay, which is a probe-based single-cell transcriptomic platform, limited our ability to detect non-coding RNAs and novel transcripts not included in the predefined probe set. Future work using whole-transcriptome approaches may uncover additional regulatory mechanisms underlying the observed effects.

In summary, this study marks a significant advance as the first to present single-cell RNA sequencing data from the adolescent midbrain following neonatal morphine exposure and probiotic intervention. Using a murine model, we demonstrated that neonatal morphine exposure profoundly disrupted cell-type-specific gene expression, canonical signaling pathways, and intercellular communication within the adolescent midbrain. Notably, probiotic supplementation with *B. infantis* effectively reversed many of these morphine-induced alterations, including the downregulation of Hox genes across multiple cell types and the activation of neuropathic pain signaling pathways. These findings offer unprecedented molecular and cellular insights into the long-term neurodevelopmental effects of early opioid exposure. Furthermore, they highlight the therapeutic potential of microbiome-targeted interventions as a promising strategy to counteract opioid-induced molecular reprogramming and promote neurodevelopmental resilience, opening new avenues for treating early-life opioid-related deficits.

Methods

Animals

Adult male and female C57BL/6 J mice (8–10 weeks old; The Jackson Laboratory, Bar Harbor, ME, USA) were used to generate experimental litters. Breeding pairs were housed in a temperature- and humidity-controlled environment under a 12-h light/dark cycle with ad libitum access to food and water. No more than five animals were housed per cage, and bedding was replaced regularly. Experimental groups were housed and handled separately to prevent cross-contamination of microbiota. Sample size was determined by power analysis (80% power, $\alpha = 0.05$) based on preliminary data, indicating a minimum of four animals per group. Only female offspring were used in this study. Animals were euthanized using CO_2 inhalation prior to tissue collection. All procedures were approved by the University of Miami Institutional Animal Care and Use Committee (IACUC) and conformed to NIH guidelines. We have complied with all relevant ethical regulations for animal use.

Neonatal morphine exposure

Nulliparous female mice (10–12 weeks old) were housed with age-matched males (4 females:1 male) for timed mating. Pregnancy was confirmed by daily monitoring and pregnant dams were housed singly. The day of birth was designated as postnatal day 0 (P0). On postnatal days 6 or 7, pups were randomly assigned to receive either morphine sulfate (5 mg/kg/day, subcutaneous; NME group) or sterile saline (control group) for five consecutive days. All injections were administered in a total volume of 10 µL once daily. In the NICU, administration schedules of morphine to infants and children vary and may continuously be updated depending on the case such as for neonatal opioid withdrawal, sedation while ventilated, short-term pain relief and severe or sustained pain. Gian M Pacifici[48] highlights the different administration schedules in each case. For instance, to train pain, children aged 1 to 5 months in the NICU may initially be given 100 to 200 µg/kg daily by subcutaneous injection, with adjusted doses according to the response[49]. The morphine dose in this study was selected based on prior preclinical reports demonstrating that the lowest morphine dose to provide analgesic efficacy in neonate rodents is 3 mg/kg[50,51]. We avoided the excessive exposure associated with higher doses as explored in other previous preclinical studies (10–15 mg/kg)[52,53]. Thus, the 5 mg/kg dosage was used as it provided efficacy in analgesia while minimizing excessive exposure. During treatment, pups were briefly separated from the dam, weighed, and maintained on a heated pad to preserve body temperature. Pups were returned to the dam immediately following each procedure. After treatment, litters remained undisturbed with the dam until weaning at P21.

Neonatal probiotic administration

Probiotic or vehicle treatments were administered to neonatal mice concurrently with neonatal morphine exposure (NME). *B. infantis* was obtained in lyophilized powder form and reconstituted in sterile water. The solution was prepared to deliver a dose of up to 1×10^9 colony-forming units (CFU) per day, consistent with previously published protocols[54,55]. Neonatal mice received either the *B. infantis* solution or a vehicle (sterile water) once daily for five consecutive days, delivered as droplets directly into the mouth. Probiotic treatment was administered during the same postnatal period as morphine or saline exposure. Upon weaning, pups were sexed and group-housed until adolescence (4–5 weeks of age). Female adolescents were used to collect the midbrain tissues.

Tissue preparation

Tissue samples were processed following the 10x Genomics Single Cell Gene Expression Flex protocol. Briefly, dissected tissues were weighed to determine the required volume of Fixation Buffer B (1 mL per 25 mg of tissue). Tissues were finely minced on a pre-chilled glass petri dish maintained on ice to facilitate pipetting through a 1.5 mm wide-bore pipette tip. The minced tissue was resuspended in Fixation Buffer B and triturated gently using a wide-bore pipette. The suspension was transferred to a 2 mL centrifuge tube and triturated further until uniformly fragmented. Samples were incubated at 4 °C for 16–24 h to allow adequate fixation.

After fixation, samples were centrifuged at $850 \times g$ for 5 min at 4 °C. The supernatant was discarded, and the tissue pellet was washed with 2 mL of chilled phosphate-buffered saline (PBS). Following centrifugation at $850 \times g$ for 5 min at room temperature, the supernatant was removed, and the tissue pellet was resuspended in 1 mL of Quenching Buffer B on ice. The sample was centrifuged again at $850 \times g$ for 5 min, and the supernatant was discarded. The fixed tissue pellet was then prepared for downstream dissociation.

Single-cell suspension generation

Fixed tissue pellets were dissociated by adding 2 mL of pre-warmed (37 °C) Dissociation Solution. Samples were processed using an Octo Dissociator to ensure consistent and efficient dissociation. The resulting cell suspension was filtered through a 30 µm cell strainer to remove debris and undissociated tissue fragments. To maximize cell recovery, the filter was rinsed with an additional 2 mL of PBS. The filtrate was centrifuged at $850 \times g$ for 5 min, and the resulting cell pellet was resuspended in 1 mL of chilled Quenching Buffer B. Cell concentration was determined using a hemocytometer or an automated cell counter (Countess II/3 FL). Fixed single-cell suspensions were processed immediately for downstream partitioning and library preparation using the 10x Genomics Chromium GEM-X Flex Single Cell Gene Expression workflow or stored in appropriate buffers according to manufacturer recommendations.

10x genomics single-cell RNA sequencing

10x Genomics Chromium Fixed RNA Profiling was performed by the Hussman Institute for Human Genomics (HIHG) at the University of Miami. Cell suspensions were assessed using the Nexcelom Cellometer K2. The suspensions were prepped following the Chromium Fixed RNA Profiling Reagent Kits for Multiplexed Samples User Guide.

Briefly, the initial step involved attaching Probe Barcodes to fixed samples through hybridization. Subsequently, these tagged samples were divided into extremely small, nanoliter-sized compartments called Gel Beads-in-emulsion (GEMs) using a microfluidic chip. To uniquely identify the molecules within each GEM, a selection from a large set of approximately 737,000 distinct 10x GEM Barcodes was introduced separately. Inside these GEMs, probes were joined together (ligated) with a 10x GEM Barcode, ensuring that all ligated probes within the same GEM carried the same barcode. These barcoded and ligated probes then underwent a bulk pre-amplification process, followed by the creation of gene expression libraries for sequencing by Illumina NovaSeq X Plus.

scRNA-seq raw data processing

Demultiplexing, barcode processing, and single-cell gene expression matrix generation were performed using the Cell Ranger multi pipeline (v.8.0.1, 10X Genomics) with the Chromium Mouse Transcriptome Probe Set v1.0.1 and default parameters. Our dataset, comprising 13 samples, initially contained 121,856 cells. Initial processing and quality control of the scRNA-seq data were conducted using the Seurat package (v.5.0)[56] in R (v.4.1.0) and RStudio (v.2022.05) implemented in Pegasus Cluster (CentOS 7) hosted by the Institute for Data Science & Computing at University of Miami. Doublet cells were individually removed for each sample using the scDblFinder package[57]. Additionally, we filtered the cells with the following parameters: maximum percentage of mitochondrial RNA = 10, minimum number of nFeature_RNA = 250 and minimum number of nCount_RNA = 500, maximum number of nFeature_RNA = 8000 and maximum number of nCount_RNA = 35,000. Following quality control, 107,427 cells from 13 samples passed the initial QC and were retained for downstream analysis. These cells were then merged and integrated using the reciprocal PCA (RPCA) method implemented in the IntegrateLayers function of the Seurat package[56] to minimize potential batch effect across experimental conditions. The integrated data were subsequently clustered using the FindClusters function with a resolution of 0.8, resulting in 48 initial clusters. Cell type annotation was performed in R using the sc-type pipeline[58] according to the steps outlined in https://github.com/IanevskiAleksandr/sc-type. Their built-in cell marker database was used; details of which can be accessed at https://sctype.app/database.php. After cell type annotation, 13 cell types were retained for downstream analysis.

Identification of differential expressed genes (DEGs) across conditions, pathway analysis, upstream regulator analysis, and cell–cell communication analysis

Differentially expressed genes (DEGs) across conditions for all cell types were identified using the FindMarkers function in Seurat, employing a built-in Wilcoxon test with Benjamini-Hochberg correction of p-values. Genes with an absolute Log2 fold change (|Log2FC|) > 0.25 and an adjusted p value < 0.005 were considered statistically significant. These DEGs were then analyzed using QIAGEN Ingenuity Pathway Analysis (IPA)[59] for canonical pathway enrichment analysis. Fisher's exact test was used in these analyses to identify signaling and metabolic pathways significantly associated with the DEGs ($p < 0.05$). Comparison Analysis in IPA software was used to summarize multiple comparisons, and the results were visualized with R package pheatmap (v 1.0.12). Upstream regulator analysis was also performed using the DEGs within the IPA software, with upstream regulators having a p value < 0.05 considered significant. Cell–cell communication analysis was performed by CellChat R packages (v 2.1.2)[60,61]. Replicate files from each condition were aggregated prior to CellChat object creation. The default CellChatDB for mouse models was used, including secreted signaling interactions, extracellular matrix (ECM)-receptor interactions, cell-cell contact interactions, and non-protein signaling (metabolic and synaptic signaling).

Statistics and Reproducibility

A total of 13 animals were used for the single-cell sequencing. Sample sizes are as follows: Saline ($n = 4$), Morphine ($n = 5$), Morphine+Probiotics ($n = 4$). In Fig. 1D, a Kruskal-Wallis test was performed to determine if any cell type proportions differed significantly among the three conditions. Differentially expressed genes (DEGs) across conditions for all cell types were identified using the FindMarkers function in Seurat, employing a built-in Wilcoxon test with Benjamini-Hochberg correction of p-values. Genes with an absolute Log2 fold change (|Log2FC|) > 0.25 and an adjusted p-value < 0.005 were considered statistically significant. Fisher's exact test was used in IPA analyses to identify signaling and metabolic pathways significantly associated with the DEGs ($p < 0.05$).

Data availability

The raw single cell RNA sequencing data has been deposited to NCBI SRA with accession number PRJNA1260540. The processed data has been deposited to NCBI GEO with accession number GSE298919. All other data are available from the corresponding author on reasonable request.

Received: 25 July 2025; Accepted: 29 October 2025;
Published online: 10 December 2025

References

1. Hall, R. W. & Anand, K. J. Pain management in newborns. *Clin. Perinatol.* **41**, 895 (2014).
2. Fong, J., Lewis, J., Lam, M. & Kesavan, K. Developmental outcomes after opioid exposure in the fetus and neonate. *NeoReviews* **25**, e325–e337 (2024).
3. Abu, Y. & Roy, S. Prenatal opioid exposure and vulnerability to future substance use disorders in offspring. *Exp. Neurol.* **339**, 113621 (2021).
4. Grecco, G. G. & Atwood, B. K. Prenatal opioid exposure enhances responsiveness to future drug reward and alters sensitivity to pain: a review of preclinical models and contributing mechanisms. *eneuro* **7**, ENEURO.0393–20.2020 (2020).
5. Durrmeyer, X., Vutskits, L., Anand, K. J. & Rimensberger, P. C. Use of analgesic and sedative drugs in the NICU: integrating clinical trials and laboratory data. *Pediatr. Res.* **67**, 117–127 (2010).
6. Patrick, S. W. et al. Neonatal opioid withdrawal syndrome. *Pediatrics* **146**, e2020029074 (2020).
7. Semple, B. D., Blomgren, K., Gimlin, K., Ferriero, D. M. & Noble-Haeusslein, L. J. Brain development in rodents and humans: Identifying benchmarks of maturation and vulnerability to injury across species. *Prog. Neurobiol.* **106**, 1–16 (2013).
8. Antoine, D. et al. Neonatal exposure to morphine results in prolonged pain hypersensitivity during adolescence, driven by gut microbial dysbiosis and gut-brain axis-mediated inflammation. *Brain Behav. Immun.* **126**, 3–23 (2025).
9. Fillingim, R. B. & Ness, T. Sex-related hormonal influences on pain and analgesic responses. *Neurosci. Biobehav. Rev.* **24**, 485–501 (2000).
10. Chambers, C. T. et al. The prevalence of chronic pain in children and adolescents: a systematic review update and meta-analysis. *Pain* **165**, 2215–2234 (2024).
11. Kalyuzhny, A. E., Arvidsson, U., Wu, W. & Wessendorf, M. W. μ-Opioid and δ-opioid receptors are expressed in brainstem antinociceptive circuits: studies using immunocytochemistry and retrograde tract-tracing. *J. Neurosci.* **16**, 6490–6503 (1996).
12. Ossipov, M. H., Morimura, K. & Porreca, F. Descending pain modulation and chronification of pain. *Curr. Opin. Support. Palliat. Care* **8**, 143–151 (2014).
13. Hu, C. et al. CellMarker 2.0: an updated database of manually curated cell markers in human/mouse and web tools based on scRNA-seq data. *Nucleic Acids Res.* **51**, D870–D876 (2023).
14. Franzén, O., Gan, L.-M. & Björkegren, J. L. PanglaoDB: a web server for exploration of mouse and human single-cell RNA sequencing data. *Database* **2019**, baz046 (2019).
15. Yan, Y. et al. Single-cell profiling of glial cells from the mouse amygdala under opioid dependent and withdrawal states. *Iscience* **26**, 108166 (2023).

16. Wei, J. et al. Single nucleus transcriptomics of ventral midbrain identifies glial activation associated with chronic opioid use disorder. *Nat. Commun.* **14**, 5610 (2023).
17. Phan, B. N. et al. Single nuclei transcriptomics in human and non-human primate striatum in opioid use disorder. *Nat. Commun.* **15**, 878 (2024).
18. Wang, X. et al. Morphine activates neuroinflammation in a manner parallel to endotoxin. *Proc. Natl. Acad. Sci.* **109**, 6325–6330 (2012).
19. Cahill, C. M. & Taylor, A. M. Neuroinflammation—a co-occurring phenomenon linking chronic pain and opioid dependence. *Curr. Opin. Behav. Sci.* **13**, 171–177 (2017).
20. Ho, M.-F. et al. Single cell transcriptomics reveals distinct transcriptional responses to oxycodone and buprenorphine by iPSC-derived brain organoids from patients with opioid use disorder. *Mol. Psychiatry* **29**, 1636–1646 (2024).
21. Lappin, T. R., Grier, D. G., Thompson, A. & Halliday, H. L. HOX genes: seductive science, mysterious mechanisms. *Ulst. Med. J.* **75**, 23 (2006).
22. Mishra A., Modi D. Role of HOXA10 in pathologies of the endometrium. *Rev. Endocr. Metab. Disord.* **26**, 1–16 (2024).
23. Capecchi, M. R. The role of Hox genes in hindbrain development. In *Molecular and cellular approaches to neural development* (eds. Cowan, W. M. Jessell, T. M. & Zipursky, S. L.), 334–355 (New York: Oxford University Press, 1997).
24. Hubert, K. A. & Wellik, D. M. Hox genes in development and beyond. *Development* **150**, dev192476 (2023).
25. Cunningham, T. J. & Duester, G. Mechanisms of retinoic acid signalling and its roles in organ and limb development. *Nat. Rev. Mol. Cell Biol.* **16**, 110–123 (2015).
26. Philippidou, P. & Dasen, J. S. Hox genes: choreographers in neural development, architects of circuit organization. *Neuron* **80**, 12–34 (2013).
27. Gaufo G. O., Wu S., Capecchi M. R. Contribution of Hox genes to the diversity of the hindbrain sensory system. *Development* **131**, 1259–1266 (2004).
28. Holstege, J. C. et al. Loss of Hoxb8 alters spinal dorsal laminae and sensory responses in mice. *Proc. Natl. Acad. Sci.* **105**, 6338–6343 (2008).
29. Philippidou, P., Walsh, C. M., Aubin, J., Jeannotte, L. & Dasen, J. S. Sustained Hox5 gene activity is required for respiratory motor neuron development. *Nat. Neurosci.* **15**, 1636–1644 (2012).
30. Shin, M. M., Catela, C. & Dasen, J. Intrinsic control of neuronal diversity and synaptic specificity in a proprioceptive circuit. *Elife* **9**, e56374 (2020).
31. Catela, C., Chen, Y., Weng, Y., Wen, K. & Kratsios, P. Control of spinal motor neuron terminal differentiation through sustained Hoxc8 gene activity. *Elife* **11**, e70766 (2022).
32. Scheefhals, N. & MacGillavry, H. D. Functional organization of postsynaptic glutamate receptors. *Mol. Cell. Neurosci.* **91**, 82–94 (2018).
33. Jackson, D. L., Graff, C. B., Richardson, J. D. & Hargreaves, K. M. Glutamate participates in the peripheral modulation of thermal hyperalgesia in rats. *Eur. J. Pharmacol.* **284**, 321–325 (1995).
34. Zhou, S., Bonasera, L. & Carlton, S. M. Peripheral administration of NMDA, AMPA or KA results in pain behaviors in rats. *Neuroreport* **7**, 895–900 (1996).
35. Latremoliere, A. & Woolf, C. J. Central sensitization: a generator of pain hypersensitivity by central neural plasticity. *J. Pain.* **10**, 895–926 (2009).
36. Zhou, X. et al. Brain-derived neurotrophic factor and trkB signaling in parasympathetic neurons: relevance to regulating α7-containing nicotinic receptors and synaptic function. *J. Neurosci.* **24**, 4340–4350 (2004).
37. Yu, C.-G. & Yezierski, R. P. Activation of the ERK1/2 signaling cascade by excitotoxic spinal cord injury. *Mol. Brain Res.* **138**, 244–255 (2005).
38. Crown, E. D. et al. Calcium/calmodulin dependent kinase II contributes to persistent central neuropathic pain following spinal cord injury. *Pain* **153**, 710–721 (2012).
39. Crown, E. D. et al. Increases in the activated forms of ERK 1/2, p38 MAPK, and CREB are correlated with the expression of at-level mechanical allodynia following spinal cord injury. *Exp. Neurol.* **199**, 397–407 (2006).
40. Zhang, L. et al. Morphine tolerance is attenuated in germfree mice and reversed by probiotics, implicating the role of gut microbiome. *Proc. Natl. Acad. Sci.* **116**, 13523–13532 (2019).
41. Singh, S. et al. Probiotic supplementation mitigates sex-dependent nociceptive changes and gut dysbiosis induced by prenatal opioid exposure. *Gut Microbes* **17**, 2464942 (2025).
42. Cai, W. et al. The gut microbiota promotes paijn in fibromyalgia. *Neuron* **113**, 2161–2175.e13 (2025).
43. Conaway, H. H., Henning, P. & Lerner, U. H. Vitamin a metabolism, action, and role in skeletal homeostasis. *Endocr. Rev.* **34**, 766–797 (2013).
44. Kolli, U. et al. Multi-omics analysis revealing the interplay between gut microbiome and the host following opioid use. *Gut Microbes* **15**, 2246184 (2023).
45. Grizotte-Lake, M. et al. Commensals suppress intestinal epithelial cell retinoic acid synthesis to regulate interleukin-22 activity and prevent microbial dysbiosis. *Immunity* **49**, 1103–1115.e1106 (2018).
46. Woo, V. et al. Commensal segmented filamentous bacteria-derived retinoic acid primes host defense to intestinal infection. *Cell Host Microbe* **29**, 1744–1756. e1745 (2021).
47. Bonakdar, M. et al. Gut commensals expand vitamin A metabolic capacity of the mammalian host. *Cell Host Microbe* **30**, 1084–1092.e1085 (2022).
48. Pacifici, G. M. Clinical pharmacology of morphine in infants and children. *J. Pharm. Pharmacol. Res.* **4**, https://doi.org/10.31579/2693-7247/053 (2021).
49. Pacifici, G. M. Metabolism and pharmacokinetics of morphine in neonates: a review. *Clinics* **71**, 474–480 (2016).
50. Zhang, G. H. & Sweitzer, S. M. Neonatal morphine enhances nociception and decreases analgesia in young rats. *Brain Res.* **1199**, 82–90 (2008).
51. Zissen, M. H. et al. Tolerance, opioid-induced allodynia and withdrawal associated allodynia in infant and young rats. *Neuroscience* **144**, 247–262 (2007).
52. Craig, M. M. & Bajic, D. Long-term behavioral effects in a rat model of prolonged postnatal morphine exposure. *Behav. Neurosci.* **129**, 643 (2015).
53. Dunn, A. D. et al. Molecular and long-term behavioral consequences of neonatal opioid exposure and withdrawal in mice. *Front. Behav. Neurosci.* **17**, 1202099 (2023).
54. Hiraku, A. et al. Early probiotic supplementation of healthy term infants with Bifidobacterium longum subsp. infantis M-63 is safe and leads to the development of Bifidobacterium-predominant gut microbiota: a double-blind, placebo-controlled trial. *Nutrients* **15**, 1402 (2023).
55. McKernan, D., Fitzgerald, P., Dinan, T. & Cryan, J. The probiotic Bifidobacterium infantis 35624 displays visceral antinociceptive effects in the rat. *Neurogastroenterol. Motil.* **22**, 1029–e1268 (2010).
56. Hao, Y. et al. Dictionary learning for integrative, multimodal and scalable single-cell analysis. *Nat. Biotechnol.* **42**, 293–304 (2024).
57. Germain, P.-L., Lun, A., Meixide, C. G., Macnair, W. & Robinson, M. D. Doublet identification in single-cell sequencing data using scDblFinder. *f1000research* **10**, 979 (2022).
58. Ianevski, A., Giri, A. K. & Aittokallio, T. Fully-automated and ultra-fast cell-type identification using specific marker combinations from single-cell transcriptomic data. *Nat. Commun.* **13**, 1246 (2022).
59. Krämer, A., Green, J., Pollard, J.rJ. & Tugendreich, S. Causal analysis approaches in ingenuity pathway analysis. *Bioinformatics* **30**, 523–530 (2014).

60. Jin, S., Plikus, M. V. & Nie, Q. CellChat for systematic analysis of cell–cell communication from single-cell transcriptomics. *Nat. Protoc.* **20**, 180–219 (2025).
61. Jin, S. et al. Inference and analysis of cell-cell communication using CellChat. *Nat. Commun.* **12**, 1088 (2021).

Acknowledgements

We would like to thank Nicolas Alberti (University of Miami) for helping to set up the supercomputer (Pegasus Cluster) and installing packages and dependencies. We would like to thank the Institute for Data Science & Computing at the University of Miami for the service units provided by the Early Career Researcher Award (EC202303). We're grateful for the valuable feedback provided by April Mann (University of Miami) on the manuscript. Research reported in this publication was supported by the National Institute on Drug Abuse Grants: F31DA059204, R01DA044582, T32DA045734, R01DA050542, and R01DA043252.

Author contributions

Junyi Tao: Conceptualization, Software, Formal analysis, Visualization, Data curation, Writing – original draft. Danielle Antoine: Conceptualization, Writing – review & editing, Visualization, Methodology, Investigation, Resources. Richa Jalodia: Resources, Investigation. Eridania Valdes: Resources, Investigation. Sean Michael Boyles: Resources, Investigation. William Hulme: Resources, Investigation. Sabita Roy: Conceptualization, Writing – review & editing, Supervision, Funding acquisition, Conceptualization.

Competing interests

The authors declare no competing interests.

Additional information

Supplementary information The online version contains supplementary material available at https://doi.org/10.1038/s42003-025-09150-0.

Correspondence and requests for materials should be addressed to Junyi Tao or Sabita Roy.

Peer review information *Communications Biology* thanks Lauren Jantzie and Trevonn Gyles for their contribution to the peer review of this work. Primary Handling Editors: Alban Latremoliere and Joao Valente.